ELSEVIER

Thalamus & Related Systems 1 (2001) 31–38

Thalamus & Related Systems

www.elsevier.com/locate/tharel

Differential control of high-voltage activated Ca^{2+} current components by a Ca^{2+}-dependent inactivation mechanism in thalamic relay neurons

Sven Meuth, Thomas Budde*, Hans-Christian Pape

Medizinische Fakultät, Institut für Physiologie, Otto-von-Guericke-Universität, Leipziger Str. 44, D-39120 Magdeburg, Germany

Abstract

Ca^{2+}-dependent inactivation of Ca^{2+} channels represents a feedback mechanism to limit the influx of Ca^{2+} into cells. Since large Ca^{2+} transients are present in thalamocortical relay neurons and Ca^{2+}-dependent mechanisms play a pivotal role for thalamic physiology, the existence of this inactivation mechanism and the involvement of different Ca^{2+} channel subtypes was investigated. The use of subtype-specific antibodies revealed the expression of α1A–α1E channel proteins on the cell body and proximal dendrites of acutely isolated cells from the rat dorsolateral geniculate nucleus (dLGN). In addition, subtype-specific channel blocking agents were used in whole cell patch clamp experiments: nifedipine (1–5 μM; L-type) blocked 35 ± 3%, ω-conotoxin GVIA (1 μM; N-type) blocked 27 ± 8%, and ω-conotoxin MVIIC (4 μM; P/Q-type) blocked 33 ± 5% of the total HVA Ca^{2+} current. The blocker-resistant current constituted about 12 ± 3% of the total Ca^{2+} current. The degree of Ca^{2+} current inactivation was assessed by using a two-pulse protocol. Under control conditions the post-pulse *I/V* was U-shaped with 35 ± 4% of the current undergoing inactivation. Inclusion of BAPTA to the internal pipette solution reduced the degree of inactivation to 15 ± 1%. When L- and P/Q-type current was blocked, the degree of inactivation was lowered to 20 ± 2 and 27 ± 3%, respectively. In the presence of ω-agatoxin TK (35 ± 6%) and ω-conotoxin GVIA (32 ± 1%) there was no change in inactivation. These data suggest that Ca^{2+}-dependent inactivation is involved in the fine tuning of Ca^{2+} entry into relay neurons mediated by L- and Q-type channels locally operated by Ca^{2+} beneath the plasma membrane.

Keywords: Ca^{2+} channel blocker; Immunocytochemistry; Patch clamp; Acutely isolated cells; Ca^{2+} domain

1. Introduction

Thalamic relay neurons possess both low-voltage activated (LVA) and high-voltage activated (HVA) Ca^{2+} currents (Hernandez-Cruz and Pape, 1989). LVA channels have been well characterized and their involvement in physiological sleep oscillations and pathophysiological epileptic activity has been recognized for a long time (Huguenard, 1996). LVA Ca^{2+} channels are activated by depolarization from hyperpolarized membrane potentials and trigger bursts of action potentials (Llinas and Jahnsen, 1982; McCormick and Bal, 1997). During wakefulness thalamic relay neurons are depolarized and LVA Ca^{2+} channels are inactivated (McCormick and Bal, 1997; Steriade, 1991). Under these conditions thalamic relay neurons fire tonic sequences of Na^+/K^+-mediated action potentials accompanied by the activation of solely HVA Ca^{2+} currents. This activity mode allows the faithful transfer of sensory information from the periphery to the cerebral cortex (relay mode). However, only little is known about HVA Ca^{2+} channels and their role in thalamic physiology. Studies combining electrophysiological and Ca^{2+} imaging techniques revealed strong increases in the intracellular Ca^{2+} concentration following HVA Ca^{2+} current activation (Munsch et al., 1997; Pedroarena and Llinas, 1997; Zhou et al., 1997). Only very recently it has been shown that HVA Ca^{2+} currents support the relay mode of thalamic relay neurons by inducing release of Ca^{2+} from intracellular stores (Budde et al., 2000). Since an excessive increase in the intracellular Ca^{2+} concentration is harmful to most cell types (Choi, 1994), relay neurons are expected to possess mechanisms restricting the entry of Ca^{2+} into the cytoplasm. A classical negative feedback mechanism between Ca^{2+} entry and intracellular Ca^{2+} concentration is provided by the Ca^{2+}-dependent inactivation of Ca^{2+} currents (Brehm and Eckert, 1978). The precise mechanism whereby Ca^{2+} entry mediates the inactivation of Ca^{2+} channels is not known. Evidence for the existence of multiple mechanisms including activation of calmodulin (Lee et al., 1999; Peterson et al., 1999; Zühlke et al., 1999), channel dephosphorylation (Armstrong, 1989), endogenous Ca^{2+} buffering (Nagerl et al., 2000), and rearrangement of the cytoskeleton (Galli and DeFelice, 1994) has been presented.

* Corresponding author. Tel.: +49-391-671-5899; fax: +49-391-671-5819.
E-mail address: thomas.budde@medizin.uni-magdeburg.de (T. Budde).

1472-9288/01/$ – see front matter
PII: S1472-9288(01)00006-1

Neurons generally have several types of HVA Ca^{2+} currents (for review see: Catterall, 1998; Striessnig, 1999). On the single cell level, they can be distinguished most clearly by their pharmacology and immunoreactivity. CNS neurons typically have L-type (α1 subunit isoforms: α1C, α1D, α1S, α1F; selective blocker: dihydropyridines), N-type (α1B; ω-conotoxin GVIA), P/Q-type (α1A; ω-conotoxin MVIIC, ω-agatoxin TK), and R-type (α1E; SNX-482) Ca^{2+} channels. All types of currents have been shown to exist in relay neurons of the ventrobasal thalamic complex (Kammermeier and Jones, 1997). HVA Ca^{2+} channel types that have been demonstrated to display Ca^{2+}-dependent inactivation are L-, N-, and P/Q-type channels (De Leon et al., 1995; Lee et al., 1999; Zeilhofer et al., 2000).

The present study was undertaken to evaluate the existence of Ca^{2+}-dependent inactivation in thalamic relay neurons, and to identify the channel subtypes mediating this mechanism.

2. Methods and techniques

2.1. Preparation

Long Evans rats (postnatal days 12–20) were deeply anaesthetized with halothane and decapitated. A block of tissue containing the rat dorsolateral geniculate nucleus (dLGN) was removed and placed in ice cold saline, containing (mM): sucrose, 210; PIPES, 20; KCl, 2.4; $MgCl_2$, 10; $CaCl_2$, 0.5; dextrose, 10; pH 7.25 with NaOH. Thalamic slices including the dLGN were prepared as coronal sections on a vibratome (Model 1000, Ted Pella, Redding, CA, USA). dLGN tissue was transferred to a spinner flask, warmed stepwise from 5 to 30°C, and incubated for 25–30 min at 30°C in an oyxgenated solution containing trypsin (0.5–1 mg/ml, Sigma, Deisenhofen, Germany) and (mM): NaCl, 120; KCl, 5; $MgCl_2$, 3; $CaCl_2$, 1; PIPES, 20; dextrose, 25; pH adjusted to 7.35 with NaOH. After washing with enzyme-free solution, slices were allowed to cool down to room temperature. Single neurons were dissociated by triturating a slice with a series of fire polished Pasteur pipettes of decreasing tip diameter.

2.2. Electrophysiology

Isolated thalamic cells were placed under an inverted microscope (Axiovert 135, Zeiss, Jena, Germany) and allowed to settle down for 20 min and perfused with a HEPES buffered solution containing (mM): NaCl, 135; KCl, 2; HEPES, 10; dextrose, 15, D-mannitol, 15; $MgCl_2$, 3; $CaCl_2$, 2; pH 7.35 with NaOH. Whole-cell recordings were performed at room temperature (21–23°C) using borosilicate glass pipettes (GC150TF-10, Clark Electromedical Instruments, Pangbourne, UK) connected to an EPC-7 amplifier (List Medical Systems, Darmstadt, Germany). Typical electrode resistance was 2–5 MΩ, with access resistance in the range 3–8 MΩ. Series resistance compensation >40% was routinely used. Voltage clamp experiments were governed by pClamp software, operating via an interface (Digidata 1200, both from Axon Instruments, Foster City, CA, USA) on an IBM AT computer. If not stated otherwise the holding potential was set to −50 mV. In order to record membrane calcium currents, the following solutions were used: (i) extracellular solution (mM): NaCl, 112; CsCl, 4; KCl, 1; HEPES, 10; dextrose, 10, $MgCl_2$, 1; $CaCl_2$, 5.0; TTX, 0.001; TEA-Cl, 20; 4-AP, 6; pH 7.35 with NaOH; (ii) intracellular solution: Cs-gluconate, 85; Cs_3-citrate, 10; NaCl, 10; KCl, 1; EGTA, 1.1; $CaCl_2$, 0.1; $MgCl_2$, 0.25; HEPES, 10; TEA-Cl, 15; Mg-ATP, 3; Na_2-GTP, 0.5; pH 7.25 with CsOH.

Data are given as mean ± S.E.M. Statistical significance was tested using a modified *t*-test for small samples. The time course of inactivation of inward currents was described by approximating the current wave form to the function

$$I = A_0 + A_1 \exp\left(-\frac{t}{\tau_1}\right) + A_2 \exp\left(-\frac{t}{\tau_2}\right) + \cdots$$

where amplitude coefficients and time constants of current decay are A_0 to A_n and τ_1 to τ_n, respectively.

2.3. Drugs

Toxins (ω-agatoxin TK, ω-conotoxin GVIA, ω-conotoxin MVIIC) were obtained from Alomone Labs (Jerusalem, Israel). Nifedipine (N7634) was obtained from Sigma. Drugs were delivered using a multi-barreled fast application system.

2.4. Immunocytochemistry

Staining was performed using procedures modified from that described previously (Budde and White, 1998). Neurons were isolated using a papain (1 mg/ml) based isolation procedure. Briefly, a suspension of isolated dLGN cells was poured upon poly-L-lysine-coated glass slides and cells were allowed to settle down for 1 h. Fixation was achieved by incubating the cells in a phosphate-buffered physiological saline (PBS, pH 7.4) containing 0.4% glutare aldehyde for 10 min. Endogenous peroxidases were inactivated by the use of H_2O_2 (0.3%, 20 min). Preincubation with normal goat serum (Sigma, 1 h, 10% diluted in PBS containing 0.3% Triton X-100) was followed by the primary antiserum against Ca^{2+} channel α1 subunits (α1A–α1E; Alomone Labs; 18 h at RT, 1:200), the secondary antiserum of biotinylated goat anti-rabbit IgG (Vector Labs, BA-5000, 1.5 h, 1:200), and the avidin–biotin-complexed horseradish peroxidase (Vector Labs, PK 4000, 1:100, 1.5 h). Between steps, slides were rinsed three times in PBS. Antibodies were diluted in PBS containing 2% goat normal serum, 0.3% Triton, 2% BSA. Enzymatic activity of the peroxidase was started by adding PBS containing 0.05% 3,3′-diaminobenzidine, 0.01% H_2O_2, 0.02% $(NH_4)_2Ni(SO_4)_2$, and 0.025% $CoCl_2$ resulting in an

enhanced dark gray to black staining of positively labeled neurons. The reaction was stopped after 10 min by infinite dilution with PBS. Slides were dehydrated and coverslipped in DePeX (Serva) mounting medium.

As a negative control, antibodies were preincubated with the control antigen peptide supplied by the manufacturer. Under these conditions no positive immunological signal could be detected. In addition, occlusion of the primary antibody from the staining procedure revealed no positive immunological signal. For each subtype antibody reactions were repeated four times.

3. Results

3.1. Identification of HVA Ca^{2+} current components in dLGN relay neurons

The expression of different HVA Ca^{2+} channel proteins in thalamic neurons was assessed by use of specific antibodies (Westenbroek et al., 1998). Neurons were isolated from the dLGN of 12–20 days old rats and only cells displaying a preserved and clear morphology after the staining procedure were used for analysis and 288–936 cells were inspected for each Ca^{2+} channel subtype. Incubation of acutely isolated dLGN neurons with an α1A-specific antiserum positively stained all investigated cells. Using previously established criteria local interneurons and relay neurons were identified (Pape et al., 1994). Both types of cells were immunopositive (Fig. 1A). Very similar results were obtained by use of antibodies specific for α1B (Fig. 1B), α1C (Fig. 1C), α1D (Fig. 1C), and α1E (Fig. 1D). The relative number of relay neurons and interneurons per object slide was 81 ± 2 and $19 \pm 2\%$ ($n = 28$), respectively. These data suggest that there is no cell type-specific or isoform-specific expression of HVA Ca^{2+} channels in rat dLGN neurons.

To determine that the expressed channel proteins were functional, dLGN relay neurons ($n = 57$) were recorded under whole cell conditions after acute isolation. Using Ca^{2+}

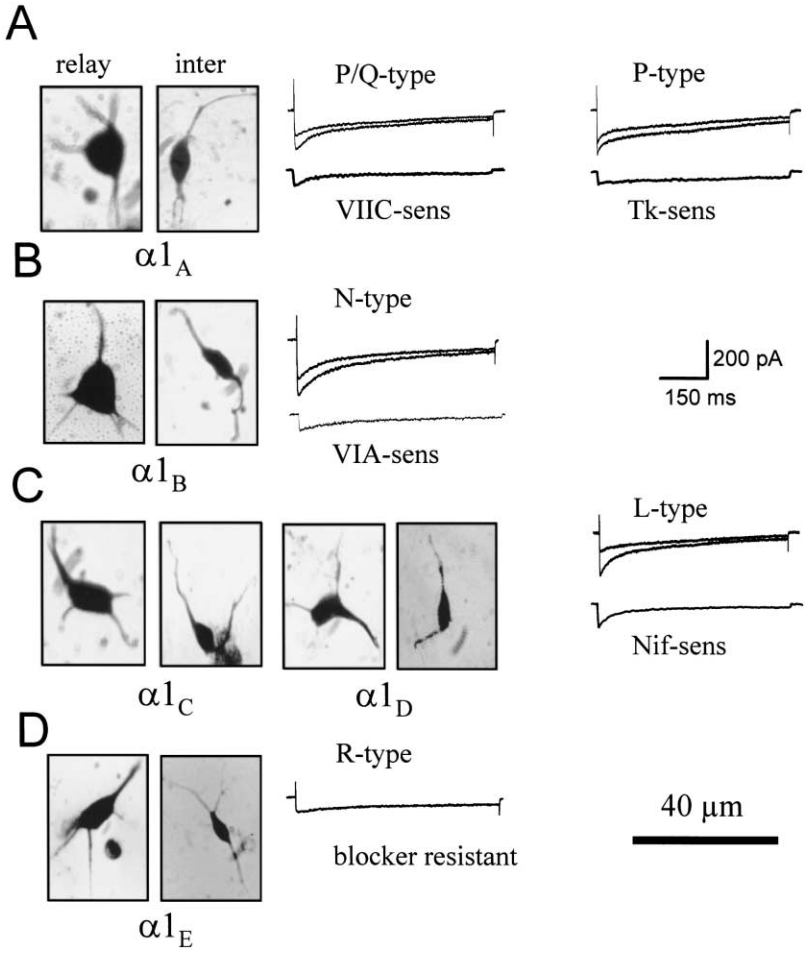

Fig. 1. Immunological and pharmacological identification of Ca^{2+} channel subtypes in dLGN neurons. Pairs of images representing relay neurons (relay, left) and interneurons (inter, right) positively stained for the presence of the Ca^{2+} channel subtype indicated beneath each pair. In addition superimposed current traces recorded under control conditions and during application of current type specific blocker are plotted on the right of the images. The corresponding blocker-sensitive component was achieved by digital subtraction for ω-conotoxin MVIIC (VIIC-sens, A), ω-agatoxin TK (TK-sens, A), ω-conotoxin GVIA (VIA-sens, B), and nifedipine (nif-sens, C). The current resistant to simultaneous application of ω-conotoxin MVIIC, ω-conotoxin GVIA, and nifedipine (resist) is shown in D. The scale bar in B and D corresponds to all current traces and cell images, respectively.

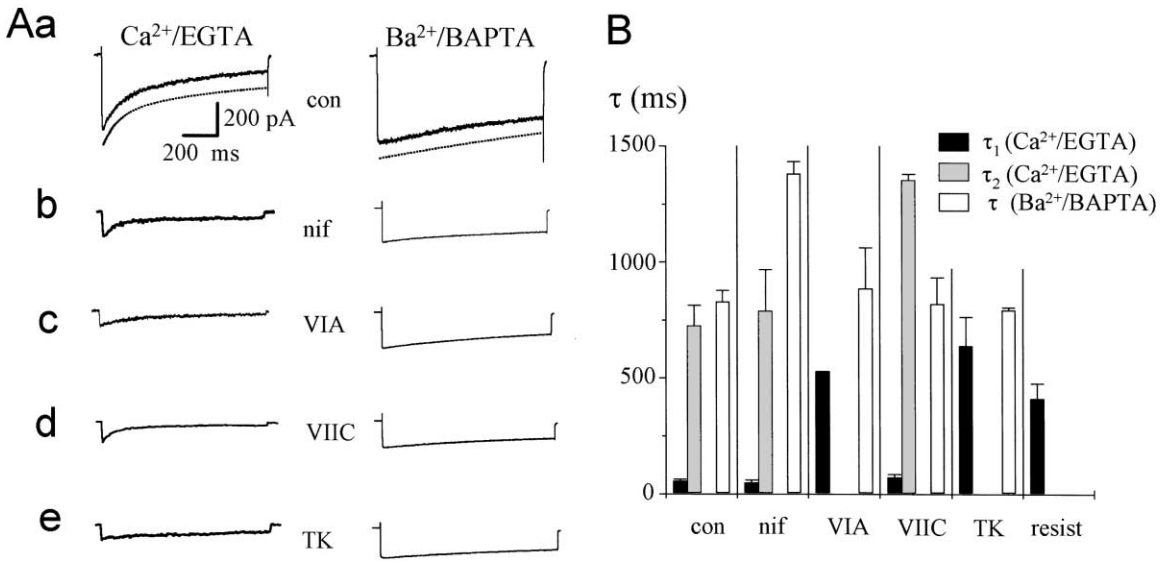

Fig. 2. Inactivation time constants of inward currents recorded with different charge carriers and intracellular Ca^{2+}-buffering. (A) Representative current traces recorded with Ca^{2+}/low EGTA (left column) and Ba^{2+}/high BAPTA (right column). Total HVA current (a) and blocker-sensitive currents are shown for nifedipine (nif; b), ω-conotoxin GVIA (VIA; c), ω-conotoxin MVIIC (VIIC; d), and; ω-agatoxin TK (TK; e). Dotted lines represent two-exponential (Ca^{2+}/EGTA: $\tau_1 = 84$ ms, $\tau_2 = 746$ ms) and single-exponential (Ba^{2+}/BAPTA: $\tau = 1386$ ms) fits to the current traces. Fits were shifted beneath current traces for clarity. (B) Bar graph representation of inactivation time constants of inward currents recorded under control conditions (con) and in the presence of the indicated blocker (abbreviations as in A). With Ca^{2+} as charge carrier two time constants of inactivation (τ_1: black bars; τ_2: gray bars) were found. With Ba^{2+} as charge carrier one time constants of inactivation (τ: white bars) was found.

as charge carrier and an intracellular recording solution with a low Ca^{2+} buffering capacity (1.1 mM EGTA), depolarization from a holding potential of −50 to +10 mV resulted in a rapidly activating inward current that notably inactivated during a 1000–1200 ms pulse (Figs. 1 and 2Aa). To test for the presence of L-type current, the effect of the dihydropyridine (DHP) antagonist nifedipine was examined. Nifedipine (1–5 μM; $n = 7$) reduced the peak current amplitude of HVA Ca^{2+} currents by 35±3% (Fig. 1C). The DHP-sensitive current component displayed a marked time dependent inactivation with $\tau_1 = 56 \pm 6$ and $\tau_2 = 726 \pm 88$ ms, respectively ($n = 7$; Fig. 2Ab and B). The N-type specific Ca^{2+} current blocker ω-conotoxin GVIA (1 μM) irreversibly inhibited 27±8% ($n = 4$; Fig. 1B) of the HVA Ca^{2+} current. The ω-conotoxin GVIA-sensitive current followed a slow single exponential process with $\tau = 530 \pm 26$ ms and displayed only little time-dependent inactivation ($n = 4$; Fig. 2Ac and B). Furthermore, 33 ± 5% ($n = 4$) of the total HVA Ca^{2+} current was blocked by ω-conotoxin MVIIC (4 μM), indicating mediation by a P/Q-type current (Fig. 1A). The ω-conotoxin MVIIC-sensitive current component displayed a marked time dependent inactivation with $\tau_1 = 72 \pm 13$ and $\tau_2 = 1350 \pm 26$ ms, respectively ($n = 4$; Fig. 2Ad and B). As the current sensitive to ω-conotoxin MVIIC could be either P- or Q-type, the funnel web spider toxin ω-agatoxin TK, a potent and selective P-type current blocker (Teramoto et al., 1993; Dobrev et al., 1998), was used next. Application of 0.1 μM ω-agatoxin TK blocked 15 ± 4% ($n = 4$) of the total HVA Ca^{2+} current, indicating that about 45% of the ω-conotoxin MVIIC-sensitive current consisted of P-type channels (Fig. 1A). The ω-agatoxin TK-sensitive component followed a single exponential time function $\tau = 700 \pm 124$ ms ($n = 3$; Fig. 2Ae and B). The R-type current component which was resistant to simultaneous application of nifedipine, ω-conotoxin GVIA, and ω-conotoxin MVIIC, accounted for 12 ± 3% ($n = 3$) of the total HVA Ca^{2+} current and revealed only little time dependent inactivation (Fig. 1D). The current followed a single exponential time course with $\tau = 450 \pm 65$ ms (Fig. 2B).

To assess whether the time-dependent inactivation of HVA current components was based on a Ca^{2+}-dependent mechanism, the blocker-specific currents were investigated after prevention of Ca^{2+}-dependent inactivation by using BAPTA (11 mM) as intracellular Ca^{2+} chelator and Ba^{2+} as main charge carrier (2Aa). Under these conditions, the total HVA Ca^{2+} current and blocker-sensitive current components were typically increased in amplitude and inactivated much slower (Fig. 2A and B). All blocker-sensitive currents inactivated following a single exponential time course with $\tau = 1300 \pm 52$ ms (L-type; Fig. 2Ab and B), $\tau = 800 \pm 96$ ms (P/Q-type; Fig. 2Ad and B), and $\tau = 900 \pm 114$ ms (N-type; Fig. 2Ac and B). The ω-agatoxin TK-sensitive component was similar during both recording conditions (Ca^{2+}: $\tau = 700 \pm 124$ ms, Fig. 2Ae and B; Ba^{2+}: $\tau = 800 \pm 45$ ms; Fig. 2Ae and B). R-type current could not be detected with Ba^{2+} as charge carrier, probably due to the lower permeability of α1E channels for Ba^{2+} compared to Ca^{2+} (Bourinet et al., 1996). These findings indicate that L- and Q-type Ca^{2+} currents are the most likely candidates for a Ca^{2+}-dependent inactivation process.

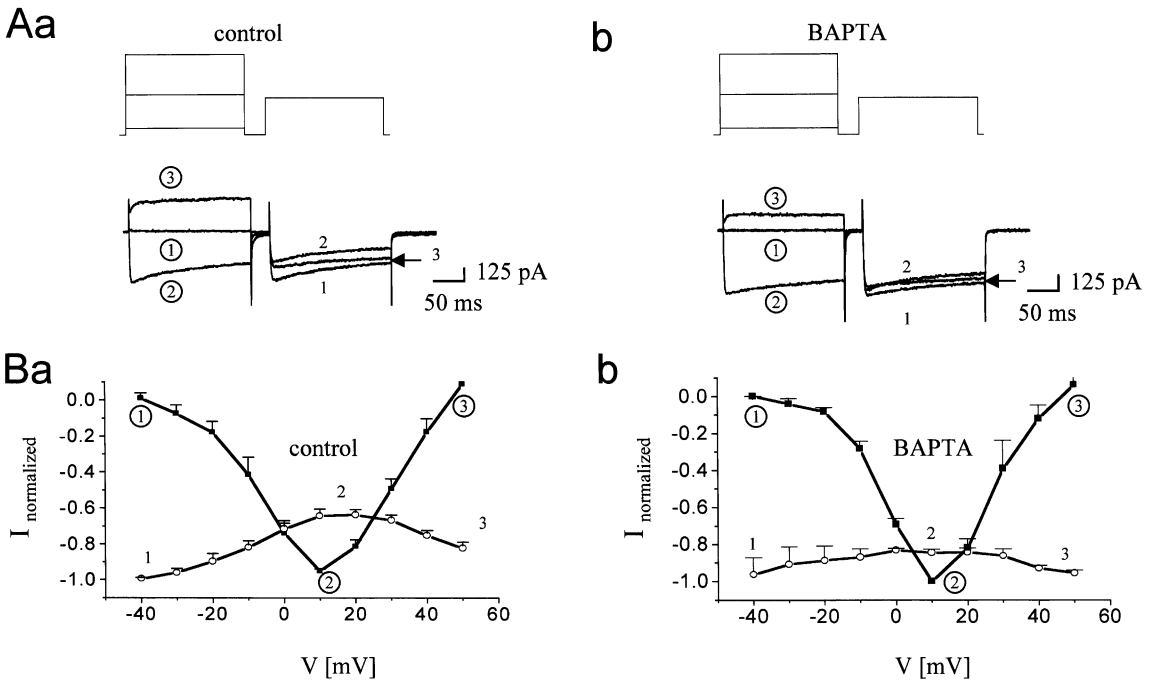

Fig. 3. Identification of Ca^{2+}-dependent inactivation by means of two-pulse protocols. (A) Representative current traces (lower panel) evoked by the indicated voltage protocol (upper panel) under control conditions (Aa) and BAPTA included to the recording pipette (Ab). A conditioning pre-pulse to varying potentials (−40 to +50 mV, 200 ms duration) was followed by a brief gap (−50 mV, 50 ms) and a subsequent analyzing post-pulse (+10 mV, 200 ms) to assess the remaining inward current. Numbers indicate corresponding pre-pulse (1–3) and post-pulse (①–③) currents. Current traces with a pre-pulse voltage of −40 (1); +10 (2); and +50 mV (3) are shown. (B) Current/voltage relationship (*I/V*) plots of currents evoked by two-pulse protocols under control conditions (Ba) and BAPTA included to the recording pipette (Bb). Pre-pulse (filled squares) and post-pulse (open circles) *I/V* are shown. Numbers correspond to the current traces in A.

To further confirm these findings, a voltage protocol was used that effectively discloses Ca^{2+}-dependent inactivation (Fig. 3A). Conditioning pre-pulses of varying potential (−40 to +50 mV, 200 ms duration) were applied followed by a brief gap (−50 mV, 50 ms) and a subsequent fixed post-pulse (+10 mV, 200 ms). The remaining HVA Ca^{2+} current under control conditions (Fig. 3Aa) and with BAPTA (11 mM) in the pipette solution (Fig. 3Ab) was analyzed. If Ca^{2+}-dependent inactivation is operative, the current evoked by the post-pulse should exhibit a U-shaped dependence on the pre-pulse potential, with maximal inactivation occurring at the peak of the *I/V* relationship where the influx of Ca^{2+} is maximal (due to normalization the post-pulse *I/V* has an inverted U-shape in the present paper and is, therefore, referred as such in the following). Under control conditions the pre-pulse *I/V* demonstrated HVA Ca^{2+} currents with an activation threshold ≤ -30 mV, maximal inward current at around +10 mV, and apparent reversal potential at around +50 mV (Fig. 3Ba, closed squares; $n = 17$). The post-pulse *I/V* (post-pulse current peak amplitude plotted versus pre-pulse voltage) was inverted U-shaped with minimal current occurring at +10 mV (35 ± 4% reduction compared to the post-pulse current evoked following a prepulse to −40 mV, $n = 17$; Figs. 2Ba (open circles) and 4B), as expected for a Ca^{2+}-dependent inactivation mechanism. The inverted U-shaped post-pulse *I/V* was obtained with a pre-pulse at +50 mV followed by 10 mV decrements and a prepulse at −40 mV followed by 10 mV increments. With BAPTA included to the internal pipette solution, time-dependent inactivation (Fig. 2B) and inverted U-shape of the post-pulse *I/V* (Fig. 3Bb, open circles) were substantially reduced. On average, the degree of inactivation was reduced to 15 ± 1% ($n = 5$; Fig. 4B).

To further assess the contribution of different HVA Ca^{2+} current components to the degree of Ca^{2+}-dependent inactivation, two-pulse protocols were delivered in the presence of subtype-specific blockers. As expected from the time-dependent inactivation of nifedipine-sensitive currents, the inverted U-shape of the post-pulse *I/V* was most effected by blocking L-type current. In the presence of 5 μM nifedipine the degree of inactivation was significantly reduced to 20 ± 2% ($n = 5$; Fig. 4Aa and B). These data indicated a clear contribution of L-type channels to Ca^{2+}-dependent inactivation in dLGN relay neurons. P/Q-type channels also contributed to Ca^{2+}-dependent inactivation, since addition of ω-conotoxin GVIIC to the extracellular solution resulted in a significant reduction of the degree of inactivation to 27 ± 3% ($n = 6$; Fig. 4Ac and B). In the presence of ω-agatoxin TK, the inverted U-shaped post-pulse *I/V* was not significantly changed, revealing a degree of inactivation of 35 ± 6% ($n = 4$; Fig. 4Ad and B). Similarly, when the

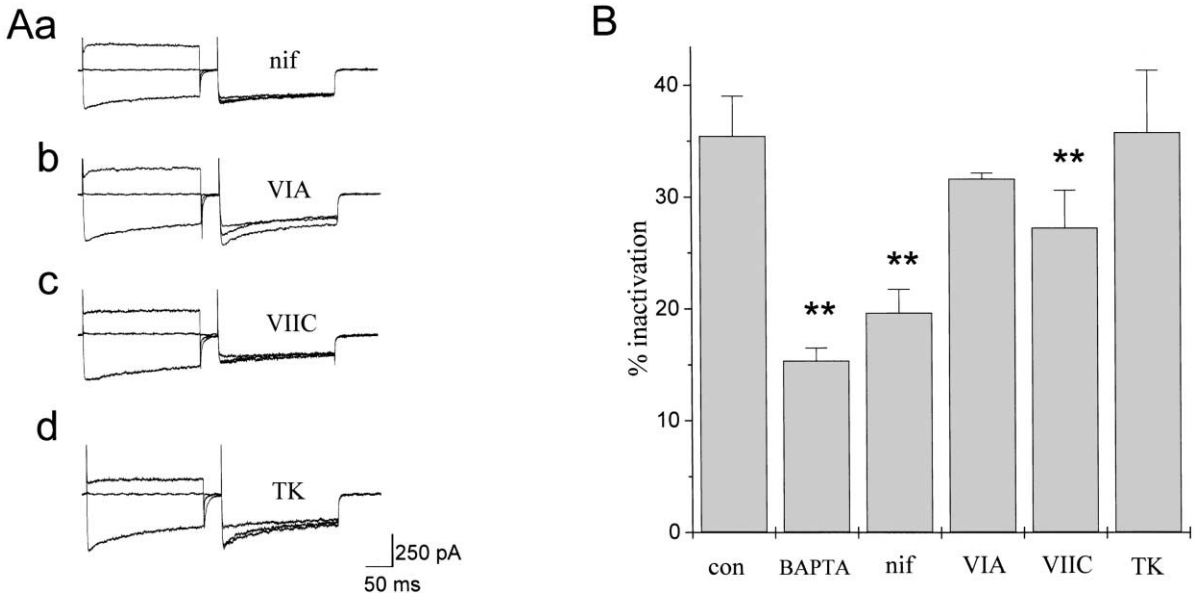

Fig. 4. Identification of Ca^{2+} current components contributing to Ca^{2+}-dependent inactivation. (A) Two-pulse protocols recorded in the presence of nifedipine (nif, a), ω-conotoxin GVIA (VIA, b), ω-conotoxin MVIIC (VIIC, c), and ω-agatoxin TK (TK, d) are shown. (B) Bar graph representation of the degree of inactivation found under control conditions (con) or in the presence of the indicated blocker (abbreviations as in A). The degree of inactivation was given by the $I_{normalized}$ values of the mean post-pulse *I/V* at +10 mV ('**' indicates $P < 0.01$).

N-type-specific blocker ω-conotoxin GVIA was used, the degree of inactivation was $32 \pm 1\%$ ($n = 5$), and not significantly different from control conditions (Fig. 4Ab and B). When the blocker-resistant current was analyzed the degree of inactivation was reduced to $3.8 \pm 0.8\%$ (data not shown), indicating that R-type current did not contribute to Ca^{2+}-dependent inactivation.

To verify that the reduction of the degree of Ca^{2+}-dependent inactivation by some of the Ca^{2+} channel blockers was not due to the decrease in Ca^{2+} current amplitude, relay neurons were perfused with extracellular solutions containing different Ca^{2+} concentrations. Changing the extracellular Ca^{2+} concentration from 5 to 3 mM resulted in a 30% reduction of the current amplitude at +10 mV from 369 ± 62 to 261 ± 19 pA ($n = 4$; data not shown). Despite this reduction in total current amplitude, the degree of Ca^{2+}-dependent inactivation was $35 \pm 2\%$ ($n = 4$), and therefore, not different from the degree of inactivation with 5 mM extracellular Ca^{2+} ($35 \pm 4\%$; $n = 17$). Furthermore, the two time constants of inactivation ($\tau_1 = 57 \pm 9$ and $\tau_2 = 628 \pm 73$ ms; $n = 4$) were very similar to the those found with 5 mM extracellular Ca^{2+} ($\tau_1 = 56 \pm 6$ and $\tau_2 = 726 \pm 88$ ms; $n = 7$).

4. Discussion

The present study was undertaken to investigate Ca^{2+}-dependent inactivation of HVA Ca^{2+} currents in dLGN relay neurons, and to identify the types of Ca^{2+} currents mediating this effect.

4.1. Pharmacological and immunocytochemical characterization of Ca^{2+} channels

Our whole-cell patch-clamp studies of dLGN relay neurons demonstrated that these cells express Ca^{2+} channels that are sensitive to dihydropyridines, ω-conotoxin GVIA, ω-agatoxin TK, and ω-conotoxin MVIIC along with a current that was resistant to these agents. These findings are consistent with the expression of α1A–α1E subunits in the cell body and proximal dendrites, as demonstrated by the use of antibodies known to specifically label class A–E α1 subunits (Westenbroek et al., 1998): (1) the expression of the α1A gene product was confirmed by the blocking effect of the P/Q-type blocker ω-conotoxin MVIIC and the P-type blocker ω-agatoxin TK (Teramoto et al., 1993; Dobrev et al., 1998); (2) the reduction of HVA Ca^{2+} currents by ω-conotoxin GVIA was well correlated with the expression of α1B protein in the cell body of dLGN relay neurons; (3) the expression of α1C and α1D channels is in agreement with the block of HVA Ca^{2+} currents by nifedipine; (4) the expression of the α1E gene was corroborated by the presence of a current component resistant to all standard blocking agents. These findings are in agreement with previous investigations of Ca^{2+} channels in thalamic neurons (for an overview see Table 1 in Kammermeier and Jones, 1997; Pedroarena and Llinas, 1997).

4.2. Mechanism of inactivation

A number of criteria have been suggested that demonstrate the presence of Ca^{2+}-dependent inactivation: (1)

Ca^{2+}-dependent inactivation should be influenced by the charge carrier used, with Ca^{2+} being more effective than Ba^{2+}. In the present study, the rate of inactivation was significantly reduced when Ba^{2+} was used as charge carrier; (2) Ca^{2+}-dependent inactivation should be reduced by introducing Ca^{2+} buffers via the patch pipette. Indeed, inclusion of 11 mM BAPTA into the recording pipette resulted in a significant reduction of the inactivation rate as well as the degree of inactivation measured in double pulse experiments; (3) in double pulse experiments, the degree of inactivation during the test pulse had an inverted U-shaped dependence on the prepulse potential, displaying a strong reduction as the prepulse potential approaches the reversal potential of Ca^{2+} currents. Taken together these findings clearly indicate the presence of a Ca^{2+}-dependent inactivation mechanism in dLGN relay neurons.

The identification of the HVA Ca^{2+} channel subtypes involved in the Ca^{2+}-dependent inactivation process was based on an analysis of the inactivation rate of the blocker-sensitive current components and the degree of inactivation measured in double pulse experiments when Ca^{2+} channel blockers were present. The following lines of evidence indicate that L- and Q-type currents are involved in Ca^{2+}-dependent inactivation: (1) currents through HVA channels were compared under conditions allowing (1.1 mM EGTA intracellular, Ca^{2+} as charge carrier) or excluding (11 mM BAPTA intracellular, Ba^{2+} as charge carrier) Ca^{2+}-dependent inactivation. Time constants of inactivation were calculated for both recording conditions. With EGTA/Ca^{2+}, only L- and P/Q-type currents revealed two time constants of inactivation, a prominent fast and a smaller slow component. When BAPTA/Ba^{2+} was used the rate of inactivation of all current components was reduced. Most noticeable was the complete block of the fast component of L- and P/Q-type currents; (2) mere blockade of L- and P/Q-type currents resulted in significant reduction of the inverted U-shape of the postpulse *I*/*V*; (3) the use of ω-agatoxin TK, a selective P-type blocker, indicated that only the Q-type component was involved in Ca^{2+}-dependent inactivation.

Two models of Ca^{2+}-dependent inactivation have previously been proposed (Sherman et al., 1990). In a shell mechanism, inactivation is affected by the Ca^{2+} concentration in a macroscopic shell beneath the plasma membrane, with the elevated Ca^{2+} concentration inactivating both open and closed channels. In the domain mechanism, only open channels interact with Ca^{2+} and thereby enter the inactivated state. Intracellular Ca^{2+} chelators should reduce the inactivation in a shell operated mechanism, but will have little effect on a domain model (Kay, 1991). In dLGN relay neurons both mechanisms seem to be operative: (1) the finding that blockade of a main HVA current component by ω-conotoxin GVIA (N-type, ∼27%) and ω-agatoxin TK (P-type, ∼15%) did not change the inverted U-shape of the inactivation curve, whereas blockade of other components (∼35%, L-type current; P/Q-type, ∼33%) did, are in agreement with a domain model: only open channels that possess a Ca^{2+}-dependent inactivation mechanism interact with Ca^{2+} passing the conducting pore and enter the inactivated state. This interpretation is corroborated by the finding that an overall reduction of the total HVA current by 30% by lowering the extracellular Ca^{2+} concentration did not reduce the degree or time course of inactivation; (2) the finding that intracellular BAPTA substantially reduced inactivation, is in agreement with a shell model (Kay, 1991). Two observations may account for this duality: (a) modeling studies of neurotransmitter release suggest that simultaneous opening of closely spaced Ca^{2+} channels near to a release site lead to overlapping Ca^{2+} microdomains and an increased probability of Ca^{2+}-dependent vesicle fusion, a phenomenon termed Ca^{2+} current cooperativity (Bertram et al., 1999); (b) L-type channels are clustered at the somato-dendritic junction of dLGN relay neurons (Budde et al., 1998). Therefore, simultaneous activation of closely spaced L-type channels may result in an area of overlapping microdomains building up a shell of increased Ca^{2+} concentration beneath the channel cluster. Under these conditions individual L-type channels will no longer determine their own rate of inactivation but cooperativity is operative.

In most central neurons, N- and L-type channels are mainly located in dendritic regions and somatic regions, respectively (Westenbroek et al., 1992; Westenbroek et al., 1998). Although the exact distribution of Ca^{2+} channels in dLGN relay cells is not known, N- and L-type channels may be located remote to each other not allowing an interference between Ca^{2+} entering via N-type channels and the inactivation mechanism of L-type channels. Similar consideration may apply to the other Ca^{2+} channels with P/Q-type located predominantly in dendrites and axon terminals and R-type channels mainly present in the soma (Pedroarena and Llinas, 1997; Westenbroek et al., 1998).

4.3. Functional significance of Ca^{2+}-dependent inactivation

The functional role of HVA Ca^{2+} channels in the thalamus presently emerges from experimental data. HVA channels seem to be more important for thalamic activity during wakefulness. A number of recent studies using imaging techniques support this view. In addition to slow oscillations during sleep, thalamic relay neurons can also generate high-frequency 40 Hz oscillations during wakefulness by activating dendritic P/Q-type Ca^{2+} currents (Pedroarena and Llinas, 1997). This type of oscillation may be involved in generating visual attention and a temporal coincidence detection mechanism. Furthermore, it seems that the tonic firing mode of relay neurons, representing an important basis for sensory information processing and transfer, relies on the Ca^{2+}-dependent release of Ca^{2+} from intracellular stores via ryanodine receptors (Budde et al., 2000). This Ca^{2+}-induced Ca^{2+} release mechanism is typically coupled to Ca^{2+} entry via L-type channels in central neurons (Chavis et al., 1996). Therefore, it seems that the two HVA Ca^{2+} current com-

ponents (namely L- and P/Q-type) with known functional importance for cellular integrative processes in the thalamus during wakefulness are also modulated by a Ca^{2+}-dependent inactivation mechanism. One reason for the existence of this mechanism may be the prevention of an excessive increase of the intracellular Ca^{2+} concentration when these channels are repetitively activated during 40 Hz oscillations or tonic firing (see above). The necessity for a negative feed back mechanism may be underlined by the recent finding that L-type channels in relay neurons are facilitated by prolonged depolarization (Kammermeier and Jones, 1998). The existence of opposing mechanisms regulating the flow of Ca^{2+} through L-type channels indicates a fine tuning of Ca^{2+} entry into thalamic relay neurons. Since both mechanisms are expected to be mainly operative during the relay mode of activity, the restriction of Ca^{2+} entry by Ca^{2+}-dependent inactivation may not be solely neuroprotective but, in addition, essential for sensory information processing.

Acknowledgements

This work was supported by the Deutsche Forschungsgemeinschaft (BU 1019/4-1; S.M. was a member of the Graduiertenkolleg "biological basis of central nervous system diseases"). Thanks are due to Mrs. R. Ziegler and Mrs. A. Reupsch for excellent technical assistance.

References

Armstrong, D.L., 1989. Calcium channel regulation by calcineurin, a Ca^{2+}-activated phosphatase in mammalian brain. TINS 12s, 117–122.

Bertram, R., Smith, G.D., Sherman, A., 1999. Modeling study of the effects of overlapping Ca^{2+} microdomains on neurotransmitter release. Biophys. J. 76, 735–750.

Bourinet, E., Zamponi, G.W., Stea, A., Soong, T.W., Lewis, B.A., Jones, L.P., Yue, D.T., Snutch, T.P., 1996. The α_{1E} calcium channel exhibits permeation properties similar to low-voltage activated calcium channels. J. Neurosci. 16, 4983–4993.

Brehm, P., Eckert, R., 1978. Calcium entry leads to inactivation of calcium channel in paramecium. Science 202, 1203–1206.

Budde, T., White, J.A., 1998. The voltage-dependent conductances of rat neocortical layer I neurons. Eur. J. Neurosci. 10, 2309–2321.

Budde, T., Munsch, T., Pape, H.-C., 1998. Distribution of L-type calcium channels in rat thalamic neurons. Eur. J. Neurosci. 10, 586–597.

Budde, T., Sieg, F., Braunewell, K.H., Gundelfinger, E.D., Pape, H.C., 2000. Ca^{2+}-induced Ca^{2+} release supports the relay mode of activity in thalamocortical cells. Neuron 26, 483–492.

Catterall, W.A., 1998. Structure and function of neuronal Ca^{2+} channels and their role in neurotransmitter release. Cell Calcium 24, 307–323.

Chavis, P., Fagni, L., Lansman, J.B., Bockaert, J., 1996. Functional coupling between ryanodine receptors and L-type calcium channels in neurons. Nature 382, 719–722.

Choi, D.W., 1994. Calcium and excitotoxic neuronal injury. Ann. N.Y. Acad. Sci. 747, 162–171.

De Leon, M., Wang, Y., Jones, L., Perez-Reyes, E., Wei, X., Soong, T.W., Snutch, T.P., Yue, D.T., 1995. Essential Ca^{2+}-binding motif for Ca^{2+}-sensitive inactivation of L-type Ca^{2+} channels. Science 270, 1502–1506.

Dobrev, D., Milde, A.S., Andreas, K., Ravens, U., 1998. Voltage-activated calcium channels involved in veratridine-evoked [3H]dopamine release in rat striatal slices. Neuropharmacology 37, 973–982.

Galli, A., DeFelice, L.J., 1994. Inactivation of L-type Ca channels in embryonic chick ventricle cells: dependence on the cytoskeletal agents colchicine and taxol. Biophys. J. 67, 2296–2304.

Hernandez-Cruz, A., Pape, H.C., 1989. Identification of two calcium currents in acutely dissociated neurons from the rat lateral geniculate nucleus. J. Neurophysiol. 61, 1270–1283.

Huguenard, J.R., 1996. Low-threshold calcium currents in central nervous system neurons. Ann. Rev. Physiol. 58, 329–3248.

Kammermeier, P.J., Jones, S.W., 1997. High-voltage-activated calcium currents in neurons acutely isolated from the ventrobasal nucleus of the rat thalamus. J. Neurophysiol. 77, 465–475.

Kammermeier, P.J., Jones, S.W., 1998. Facilitation of L-type calcium current in thalamic neurons. J. Neurophysiol. 79, 410–417.

Kay, A.R., 1991. Inactivation kinetics of calcium currents of acutely dissociated CA1 pyramidal cells of the mature guinea-pig hippocampus. J. Physiol. (Lond.) 437, 27–48.

Lee, A., Wong, S.T., Gallagher, D., Li, B., Storm, D.R., Scheuer, T., Catterall, W.A., 1999. Ca^{2+}/calmodulin binds to and modulates P/Q-type calcium channels. Nature 399, 155–159.

Llinas, R., Jahnsen, H., 1982. Electrophysiology of mammalian thalamic neurones in vitro. Nature 297, 406–408.

McCormick, D.A., Bal, T., 1997. Sleep and arousal: thalamocortical mechanisms. Ann. Rev. Neurosci. 20, 185–215.

Munsch, T., Budde, T., Pape, H.-C., 1997. Voltage-activated intracellular calcium transients in thalamic relay cells and interneurons. Neuroreport 8, 2411–2418.

Nagerl, U.V., Mody, I., Jeub, M., Lie, A.A., Elger, C.E., Beck, H., 2000. Surviving granule cells of the sclerotic human hippocampus have reduced Ca(2+) influx because of a loss of calbindin-D(28k) in temporal lobe epilepsy. J. Neurosci. 20, 1831–1836.

Pape, H.C., Budde, T., Mager, R., Kisvrday, Z., 1994. Prevention of Ca^{2+}-mediated action potentials in GABAergic local circuit neurons of the thalamus by a transient K^+ current. J. Physiol. (Lond.) 478.3, 403–422.

Pedroarena, C., Llinas, R., 1997. Dendritic calcium conductances generate high-frequency oscillation in thalamocortical neurons. PNAS 94, 724–728.

Peterson, B.Z., DeMaria, C.D., Adelman, J.P., Yue, D.T., 1999. Calmodulin is the Ca^{2+} sensor for Ca^{2+}-dependent inactivation of L-type calcium channels. Neuron 22, 549–558.

Sherman, A., Keizer, J., Rinzel, J., 1990. Domain model for Ca^{2+}-inactivation of Ca^{2+} channels at low channel density. Biophys. J. 58, 985–995.

Steriade, M., 1991. Alertness, quiet sleep, dreaming. Cereb. Cortex 9, 279–357.

Striessnig, J., 1999. Pharmacology, structure and function of cardiac L-type Ca(2+) channels. Cell. Physiol. Biochem. 9, 242–269.

Teramoto, T., Kuwada, M., Niidome, T., Sawada, K., Nishizawa, Y., Katayama, K., 1993. A novel peptide from funnel web spider venom, omega-Aga-TK, selectively blocks, P-type calcium channels. Biochem. Biophys. Res. Commun. 196, 134–140.

Westenbroek, R.E., Hell, J.W., Warner, C., Dubel, S.J., Snutch, T.P., Catterall, W.A., 1992. Biochemical properties and subcellular distribution of an N-type calcium channel alpha1 subunit. Neuron 9, 1099–1115.

Westenbroek, R.E., Hoskins, L., Catterall, W.A., 1998. Localization of Ca^{2+} channel subtypes on rat spinal motor neurons, interneurons, and nerve terminals. J. Neurosci. 18, 6319–6330.

Zeilhofer, H.U., Blank, N.M., Neuhuber, W.L., Swandulla, D., 2000. Calcium-dependent inactivation of neuronal calcium channel currents is independent of calcineurin. Neuroscience 95, 235–241.

Zhou, Q., Godwin, D.W., O'Malley, D.M., Adams, P.R., 1997. Visualization of calcium influx through channels that shape the burst and tonic firing modes of thalamic relay cells. J. Neurophysiol. 77, 2816–2825.

Zühlke, R.D., Pitt, G.S., Deisseroth, K., Tsien, R.W., Reuter, H., 1999. Calmodulin supports both inactivation and facilitation of L-type calcium channels. Nature 399, 159–162.